

Supplement of

Long-term changes in black carbon and aerosol optical properties from 2012 to 2020 in Beijing, China

Jiaying Sun^{1,2}, Zhe Wang¹, Wei Zhou¹, Conghui Xie^{1,2, a}, Cheng Wu³, Chun Chen^{1,2}, Tingting Han^{1, b},
Qingqing Wang¹, Zhijie Li^{1,2}, Jie Li¹, Pingqing Fu⁴, Zifa Wang^{1,2,5}, and Yele Sun^{1,2,5 *}

¹State Key Laboratory of Atmospheric Boundary Layer Physics and Atmospheric Chemistry, Institute of Atmospheric Physics, Chinese Academy of Sciences, Beijing 100029, China

²College of Earth and Planetary Sciences, University of Chinese Academy of Sciences, Beijing 100049, China

³Institute of Mass Spectrometer and Atmospheric Environment, Jinan University, Guangzhou 510632, China

⁴Institute of Surface-Earth System Science, Tianjin University, Tianjin 300072, China

⁵Center for Excellence in Regional Atmospheric Environment, Institute of Urban Environment, Chinese Academy of Sciences, Xiamen 361021, China

^anow at: State Key Joint Laboratory of Environmental Simulation and Pollution Control, College of Environmental Sciences and Engineering, Peking University, Beijing, 100871, China

^bnow at: Environmental Meteorology Forecast Center of Beijing-Tianjin-Hebei, Beijing 100089, China

* *Correspondence to:* Yele Sun (sunyele@mail.iap.ac.cn)

Table S1. A summary of Mann-Kendall trend test for air pollutants from 2013 to 2020.

	Entire	Spring	Summer	Fall	Winter
	τ	τ	τ	τ	τ
	(p-value)	(p-value)	(p-value)	(p-value)	(p-value)
eBC	-1 (0.01)	-1 (0.01)	-0.4 (0.33)	-1 (0.01)	-0.4 (0.33)
eBC/PM _{2.5}	-0.6 (0.14)	0.4 (0.33)	-0.4 (0.33)	-0.8 (0.05)	-0.8 (0.05)
eBC/CO	-0.6 (0.14)	-0.8 (0.05)	-0.4 (0.33)	-0.6 (0.14)	-0.8 (0.05)
b_{ext}	-0.8 (0.05)	-0.8 (0.05)	- -	-0.8 (0.05)	-0.4 (0.33)
SSA	1 (0.01)	- -	0.8 (0.05)	0.8 (0.05)	0.8 (0.05)
MEE	0.4 (0.33)	-0.2 (0.62)	0.8 (0.05)	- -	-0.2 (0.62)

Table S2. A summary of relationship between aerosol optical depth and light extinction coefficient measured by CAPS in four seasons.

	Entire	Spring	Summer	Fall	Winter
Effective Height (m, slope)	1233	1200	1800	964	635
r	0.64	0.66	0.76	0.72	0.72

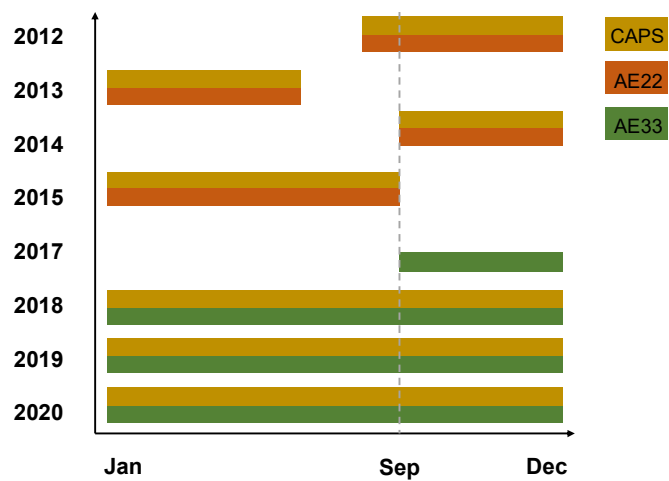


Fig. S1. Schematic representation of instrument deployment in different years.

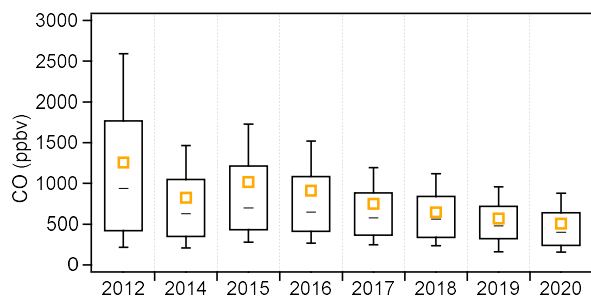


Fig. S2. Annual variation of CO concentration. The median (horizontal line), mean (square), 25th and 75th percentiles (lower and upper box), and 10th and 90th percentiles (lower and upper whiskers) are also shown, same as below.

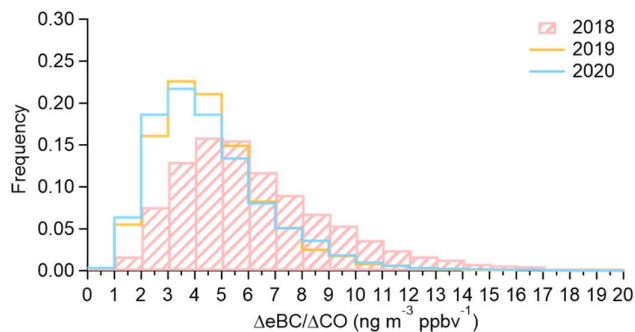


Fig. S3. The frequency distributions of $\Delta e_{BC}/\Delta CO$ in the past three years.

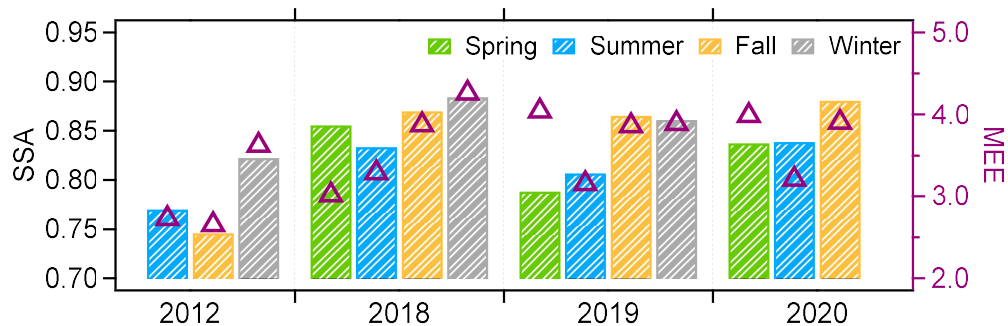


Fig. S4. Seasonal mean of SSA and MEE.

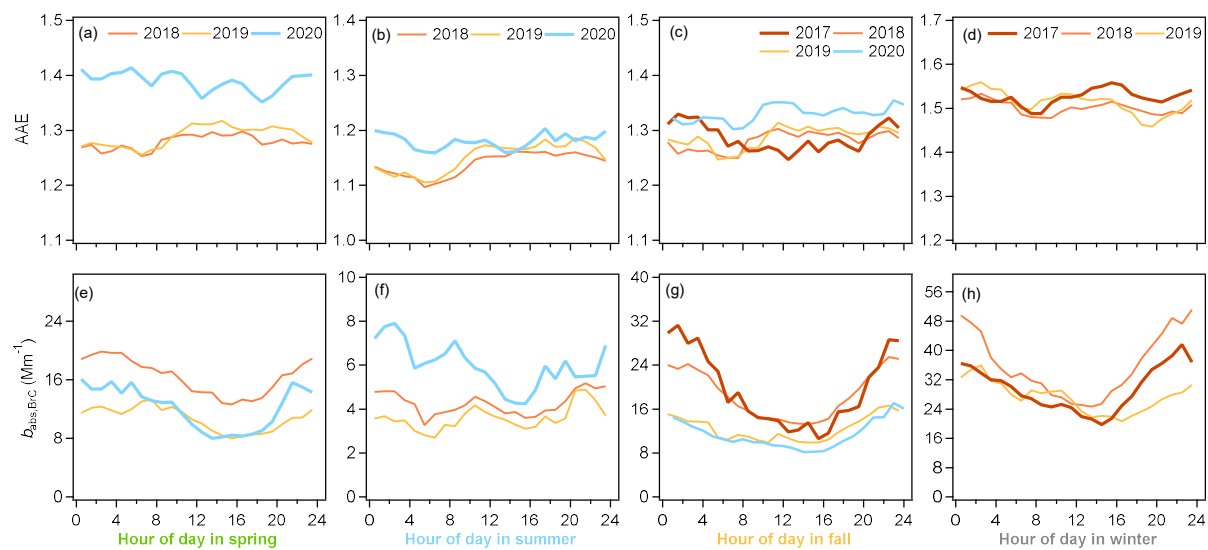


Fig. S5. Diurnal variations of AAE and $b_{abs, BrC}$ for spring, summer, fall and winter time in different years.

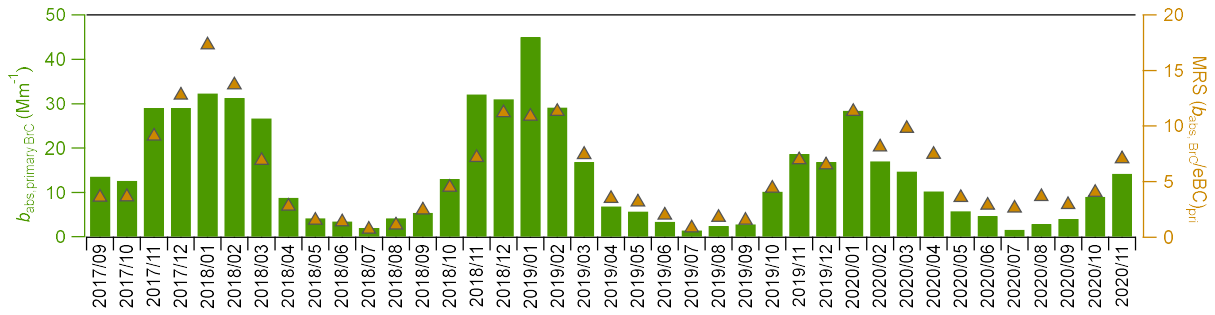


Fig. S6. Monthly variations in results of MRS and b_{abs} , primary BrC.

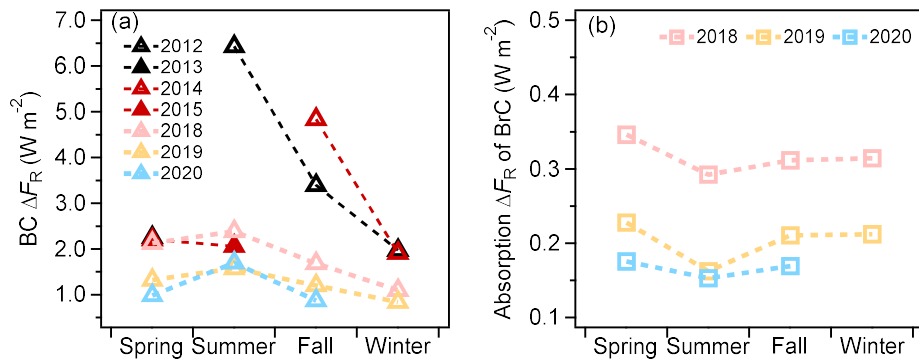


Fig. S7. Seasonal variations of $BC \Delta F_R$ and BrC absorption ΔF_R .

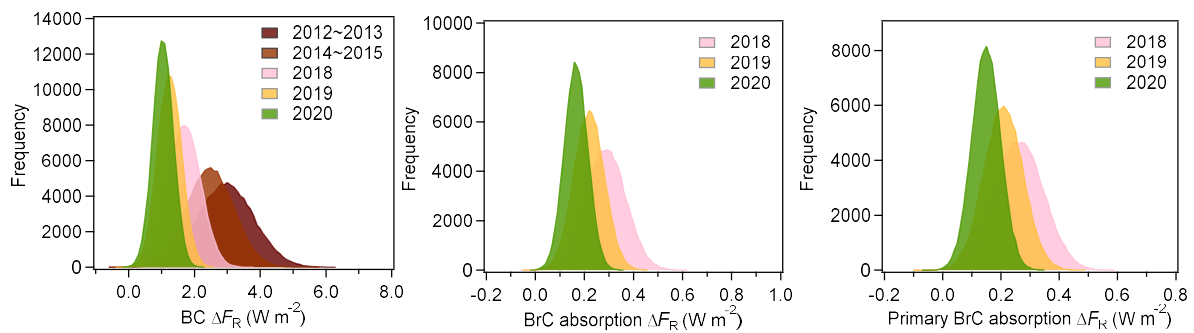


Fig. S8. Probability distributions of ΔF_R for BC, BrC and primary BrC based on 100,000 Monte Carlo simulations.